BBA - Biomembranes 1866 (2024) 184311

Contents lists available at ScienceDirect

BBA - Biomembranes

journal homepage: www.elsevier.com/locate/bbamem

Modification of the RTX domain cap by acyl chains of adapted length rules the formation of functional hemolysin pores

Anna Lepesheva [a,b,1], Michaela Grobarcikova [a,b,1], Adriana Osickova [a], David Jurnecka [a], Sarka Knoblochova [a], Monika Cizkova [a], Radim Osicka [a], Peter Sebo [a,*], Jiri Masin [a,*]

[a] Institute of Microbiology of the Czech Academy of Sciences, Prague, Czech Republic
[b] Faculty of Science, Charles University in Prague, Prague, Czech Republic

ARTICLE INFO

Keywords:
RTX toxin
Adenylate cyclase toxin
α-Hemolysin
Chimera
Fatty acylation
Cytotoxicity

ABSTRACT

The acylated pore-forming Repeats in ToXin (RTX) cytolysins α-hemolysin (HlyA) and adenylate cyclase toxin (CyaA) preferentially bind to β_2 integrins of myeloid leukocytes but can also promiscuously bind and permeabilize cells lacking the β_2 integrins. We constructed a $HlyA_{1–563}/CyaA_{860–1706}$ chimera that was acylated either by the toxin-activating acyltransferase CyaC, using sixteen carbon-long (C16) acyls, or by the HlyC acyltransferase using fourteen carbon-long (C14) acyls. Cytolysin assays with the C16- or C14-acylated HlyA/CyaA chimeric toxin revealed that the RTX domain of CyaA can functionally replace the RTX domain of HlyA only if it is modified by C16-acyls on the Lys983 residue of CyaA. The C16-monoacylated HlyA/CyaA chimera was as pore-forming and cytolytic as native HlyA, whereas the C14-acylated chimera exhibited very low pore-forming activity. Hence, the capacity of the RTX domain of CyaA to support the insertion of the N-terminal pore-forming domain into the target cell membrane, and promote formation of toxin pores, strictly depends on the modification of the Lys983 residue by an acyl chain of adapted length.

1. Introduction

Pore-forming toxins of the Repeats in ToXins (RTX) family are important virulence factors of several pathogenic Gram-negative bacteria. These toxins permeabilize host cell membranes by forming cation-selective pores that are cytotoxic to a variety of cell types [1]. The RTX adenylate cyclase toxin (CyaA, ACT, or Hly-AC) secreted by pathogenic *Bordetellae* is a 1706 residue-long polypeptide (Fig. 1A) that subverts immune cell functions [2–4]. CyaA can interact promiscuously at a low efficacy with a variety of cell types and associates about a hundred-fold more efficiently with myeloid cells expressing the $\alpha_M\beta_2$ integrin known as complement receptor 3 (CR3, CD11b/CD18, or Mac-1), which the toxin selectively binds through the α-subunit CD11b [5,6]. The RTX hemolysin moiety (Hly) of CyaA (~1300C-proximal residues) alone forms small cation-selective membrane pores [7] that permeabilize membranes of various cells [8–12] and can provoke colloid-osmotic (oncotic) lysis of erythrocytes [13]. The Hly portion of CyaA comprises an AC-to-Hly linker segment [14–18] followed by a hydrophobic pore-forming domain [19–25] and a ~ 900 residue-long calcium- and CD11b-binding RTX domain. This is capped on its N-terminus by an acylated segment that harbors two conserved lysine residues (Lys860 and Lys983) modified on ε-amino groups by palmitoyl and palmitoleyl acyls (C16:0 or C16:1) by the co-expressed toxin-activating acyltransferase CyaC [26–29]. The C-terminal RTX moiety of CyaA then consists of five blocks of calcium-binding nonapeptide repeats (Fig. 1A) that fold into five typical RTX β-roll structures interspersed by conserved β-structured linker segments [6,30–33].

Another prototypic member of the RTX cytolysin family is the α-hemolysin (HlyA, Fig. 1A), a 1024 residue-long polypeptide secreted by pathogenic and some commensal isolates of *Escherichia coli*. Activation of the proHlyA protoxin to active HlyA toxin involves covalent C14:0 myristoylation and C14:0-OH hydroxymyristoylation of the Lys564 and Lys690 residues by the cognate toxin acyltransferase HlyC [34–37]. The calcium-binding RTX domain of HlyA is much shorter than the RTX domain of CyaA (Fig. 1A) and appears to form a single β-roll structure that mediates HlyA binding to the shared CD18 subunit of β_2 integrins of leukocytes [38–42]. However, like other RTX toxins, also HlyA can promiscuously bind cells in an integrin-independent manner

* Corresponding authors.
E-mail addresses: sebo@biomed.cas.cz (P. Sebo), masin@biomed.cas.cz (J. Masin).
[1] These authors contributed equally to this work.

https://doi.org/10.1016/j.bbamem.2024.184311
Received 1 February 2024; Received in revised form 14 March 2024; Accepted 25 March 2024
Available online 1 April 2024

and permeabilizes erythrocytes and various nucleated cells by formation of toxin pores [43–46].

Both irreversible insertion into and oligomerization of the activated HlyA within the cell membrane was shown to depend on the HlyC-mediated acylation [47–49]. In line with that, the covalent amide-linked fatty acyl modification of the two conserved lysine residues (Lys860 and Lys983) of CyaA by CyaC was shown to play a structural role in the folding of the toxin molecule into its biologically active cell-invasive conformation [50–55]. Furthermore, the structure of attached acyl residues appears to modulate the propensity of CyaA molecules to oligomerize into toxin pores within cell membranes [7,28,56]. Whereas the acylation by unsaturated C16:1 palmitoyl residues confers on CyaA

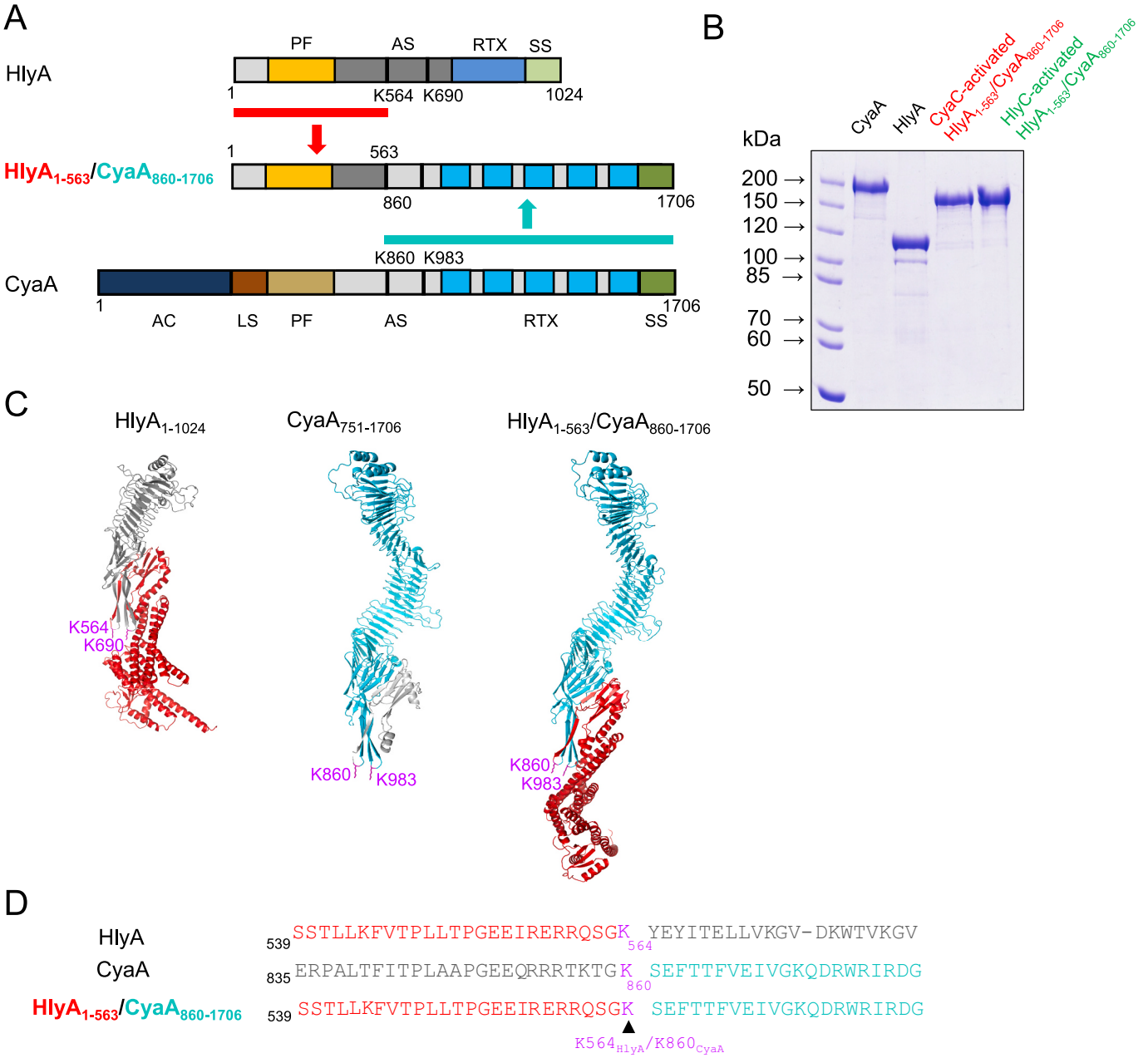

Fig. 1. Schematic representation of HlyA, CyaA, and of the $HlyA_{1-563}/CyaA_{860-1706}$ hybrid. (A) Schematic representation of functional organization of the used toxin and hybrid molecules. The individual functional domains of the HlyA and CyaA toxins are indicated by colored rectangles. AC, adenylate cyclase domain; LS, AC-to-Hly linker segment; PF, pore-forming domain; AS, acylated segment; RTX, calcium-binding repeats; SS, secretion signal. The numbers in the name of the HlyA/CyaA hybrid represent the numbers of the first and of the last residues of the fused segments of the HlyA and CyaA toxins according to the sequences of full-length HlyA and CyaA proteins, respectively. The hybrid harbors the hydrophobic domain and the N-terminal part of the acylated segment of HlyA (residues 1 to 563 of HlyA, schematically represented by a red rectangle), fused to the C-terminal part of the acylated segment and the RTX domain of CyaA (residues 860 to 1706 of CyaA, cyan rectangle). (B) The toxins were produced in *E. coli* XL-1 cells and purified from urea extracts as described under Materials and methods. Samples were analyzed on 7.5 % polyacrylamide gels and stained with Coomassie blue. (C) AlphaFold models of the structures of HlyA, of the CyaA fragment 751–1706 (PDB ID: 7USL [32]), and of the $HlyA_{1-563}/CyaA_{860-1706}$ hybrid, respectively. The gray marked portions of HlyA and CyaA were not present in the $HlyA_{1-563}/CyaA_{860-1706}$ hybrid. Residues 1 to 563 of HlyA are highlighted in red, residues 860 to 1706 of CyaA are highlighted in cyan, and the acylated lysine residues of HlyA and CyaA are highlighted in magenta. (D) The ClustalW sequence alignments of portions of the acylated segments of HlyA and CyaA. HlyA, *Escherichia coli* (NCBI reference sequence: WP_000208152.1); CyaA, *Bordetella pertussis* (WP_010929995.1). Partial sequences of the acylated segments of HlyA and CyaA are highlighted in red and cyan, respectively. Lysine residues (Lys564 of HlyA, Lys860 of CyaA, and $Lys564_{HlyA}/Lys860_{CyaA}$ of the $HlyA_{1-563}/CyaA_{860-1706}$ hybrid) are highlighted in magenta color.

the same capacity to penetrate target cell membrane and deliver the AC domain into cell cytosol as does the modification by saturated C16:0 acyls, the C16:1 acyls enable only a reduced pore-forming capacity of CyaA [7,28,56].

The molecular mechanism of formation and the structures of the HlyA and CyaA-formed pores in target cell membranes remain poorly understood. Controversies persist on their oligomer stoichiometry and involved structures [7,57–60]. Formation of the HlyA and CyaA pores was postulated to involve the predicted amphipathic and hydrophobic α-helices comprised within the ~200 residue-long segments of their pore-forming domains, namely the residues 238 to 411 of HlyA and 502 to 698 of CyaA [19,21–23,61–66]. Whereas the HlyA toxin forms pores of an estimated inner diameter of ~2 nm, CyaA forms much smaller pores of a diameter around ~0.6–0.8 nm [7,39,67–69] and CyaA exhibits a much lower specific hemolytic activity than the *bona fide* RTX hemolysin HlyA.

In the absence of structural data, a useful surrogate approach to mechanistic deciphering of the contributions of individual toxin segments to receptor and membrane interaction of the CyaA and HlyA toxins consists in the characterization of the activities of their molecular CyaA/HlyA chimeras [39]. Using structural homology predictions, segments of the two toxins can be exchanged and characterization of such chimeras enabled us previously to define the LFA-1-binding moiety of HlyA. Using this approach, we could also identify the residue 400 to 710 segment of CyaA as the "adenylate cyclase domain translocon" sufficient for translocation of the AC domain polypeptide across the plasma membrane of target cells [39]. Therefore, we employed here this approach to tackle the role of acyl chain length in the activation and membrane insertion of RTX toxins, taking advantage of the high degree of similarity between the N-terminal sequences flanking the acylated Lys564 and Lys860 residues of the HlyA and CyaA toxins (Supplementary Fig. 1). We constructed an $HlyA_{1–563}/CyaA_{860–1706}$ chimera to test the hypothesis that the RTX domain and its acylated segment (residues 860 to 1706 of CyaA) may deliver into cell membrane and might thus support the formation of cytolytic pores by an N-terminally linked pore-forming domain derived from HlyA. We show that this was the case only when the Lys983 residue of the RTX moiety of CyaA was acylated by a C16 acyl of adapted length, whereas a shorter C14 acyl conferred on the toxin chimera a much lower capacity to insert the HlyA-derived pore-forming domain into cell membrane. This work reveals the requirement for a structural match between the attached acyl chain of adapted length and the structure of the acylated RTX domain cap.

2. Material and methods

2.1. Antibodies

Monoclonal antibodies (mAbs) OKM1-Dy495 and MEM-48 APC were obtained from Exbio (Czech Republic), and M1/70 was purchased from Pharmingen (CA).

2.2. Bacterial strains

The *E. coli* strain XL1-Blue (Stratagene, La Jolla, CA) was used throughout this work for DNA manipulations and was grown in Luria-Bertani medium at 37 °C.

2.3. Cell lines

Chinese hamster ovary cells (CHO-K1, ATCC CCL-61) stably transfected with human CD11b/CD18 (CHO-CR3), CD11a/CD18 (CHO-LFA-1) or mock-transfected (CHO) were prepared previously [6] and grown in F12K medium (GIBCO Invitrogen, Grand Island, NY, USA) supplemented with 10 % FCS and antibiotic antifungal solution. Prior to WST-1 assay, F12K was replaced with D-MEM (Dulbecco's Modified Eagle Medium, 1.9 mM Ca^{2+}) without FCS and the cells were allowed to rest in D-MEM for 1 h at 37 °C in a humidified 5 % CO_2 atmosphere. Cell surface expression of CD11b and CD18 subunits was examined by flow cytometry (Supplementary Fig. 2).

2.4. Plasmid construction

For production of HlyC-activated HlyA, the pT7*hlyC-hlyA* plasmid harboring *hlyC* and *hlyA* gene, which was fused in frame at the 3′-terminus to a sequence encoding a double-hexahistidine purification tag was used [69]. The pT7CACT1 plasmid [70], harboring the *cyaC* and *cyaA* genes, was used for production of CyaA. The enzymatically inactive CyaA-AC^{-} form of the protein, unable to convert ATP to cAMP, was generated by placing a Cys-Thr dipeptide between amino acid residues Asp188 and Ile189 of the ATP-binding site in the catalytic domain of CyaA, as described previously [70]. The pT7*hlyC-hlyA* and pT7*cyaC-hlyA* plasmids [69] were used as parental plasmids to generate a construct for the expression of the $HlyA_{1–563}/CyaA_{860–1706}$ hybrid molecule activated by the acyltransferase HlyC or CyaC. For this purpose, the pT7CACT1 plasmid [70] was used as a source of the $cyaA_{860–1706}$ fragment, which was amplified by PCR and cloned instead of the $hlyA_{564–1024}$ fragment in the pT7*hlyC-hlyA* and pT7*cyaC-hlyA* plasmids. The resulting plasmids pT7*hlyC-hlyA*$_{1–563}$/*cyaA*$_{860–1706}$ and pT7*cyaC*-$hlyA_{1–563}/cyaA_{860–1706}$ were used to purify the HlyC- or CyaC-activated $HlyA_{1–563}/CyaA_{860–1706}$ hybrid molecule, respectively. To construct the plasmid pT7*hlyA*$_{1–563}$/*cyaA*$_{860–1706}$ for the expression of the non-acylated $proHlyA_{1–563}/CyaA_{860–1706}$ chimera, the *hlyC* gene was excised from the plasmid pT7*hlyC-hlyA*$_{1–563}$/*cyaA*$_{860–1706}$ using the restriction endonuclease *Xba*I.

2.5. Protein production, purification, and labeling

The intact CyaA, CyaA-AC^{-}, intact HlyA and the $HlyA_{1–563}/CyaA_{860–1706}$ hybrid molecules were produced in *E. coli* XL-1 blue cells transformed with the appropriate plasmids. For protein purification, the cells were harvested by centrifugation, washed twice with 50 mM Tris-HCl (pH 8.0), disrupted by sonication at 4 °C and the homogenate was centrifuged at 20,000 x*g* for 30 min at 4 °C. The inclusion bodies collected in the pellet were solubilized with 50 mM Tris-HCl (pH 8.0) containing 8 M urea and the urea extract was cleared at 20,000 x g for 30 min at 4 °C. The urea extract containing intact HlyA was loaded on an Ni-NTA agarose column (Qiagen, Germantown, MD) equilibrated with 50 mM Tris-HCl (pH 8.0), 200 mM NaCl and 8 M urea (TNU), washed and eluted with TNU buffer containing 600 mM imidazole. The urea extract containing CyaA was purified by combination of DEAE Sepharose and Phenyl Sepharose [14]. The extracts of $HlyA_{1–563}/CyaA_{860–1706}$ hybrids in Tris-HCl 50 mM (pH 8.0), 8 M urea were loaded on DEAE-Sepharose resin pre-equilibrated with Tris-HCl 50 mM (pH 8.0), 8 M urea. Contaminating components were removed by washing of the column with Tris-HCl 50 mM (pH 8.0), 8 M urea, 150 mM NaCl. Finally, $HlyA_{1–563}/CyaA_{860–1706}$ hybrids were eluted with Tris-HCl 50 mM (pH 8.0), 8 M urea, 200 mM NaCl. Protein labeling was performed on the Phenyl-Sepharose CL-4B column after the Ni-NTA agarose or DEAE-Sepharose purification step. Briefly, the purified protein samples were diluted 4-times in ice-cold 50 mM Tris-HCl, pH 8.0 containing 1 M NaCl and loaded on Phenyl-Sepharose CL-4B beads (Sigma–Aldrich, St. Louis, MO). The Phenyl-Sepharose column was then washed with 50 mM sodium bicarbonate (pH 8.3) containing 1 M NaCl and the beads were resuspended in the same buffer containing Dy647-NHS ester (Dyomics, Jena, Germany) in a concentration to reach a Dyomics:protein molar ratio of ~5:1. Labeling was performed at 25 °C for 2 h and the column was subsequently washed with 50 mM Tris-HCl (pH 8.0). The labeled proteins were eluted in TU buffer (50 mM Tris-HCl pH 8.0, 8 M urea). Protein concentrations were determined by Bradford assay (Bio-Rad).

2.6. Binding of Dyomics-labeled CyaA and $HlyA_{1–563}/CyaA_{860–1706}$ hybrids to cells

Washed sheep erythrocytes (5×10^5/200 μl) in TNC buffer (Tris 50 mM (pH 7.4), NaCl 150 mM, $CaCl_2$ 2 mM) supplemented with 100 mM polyethylenglycol (PEG) 1500, CHO, CHO-LFA-1 or CHO-CR3 cells (10^5/100 μl) in cold HEPES-buffered salt solution (HBSS buffer; 10 mM HEPES pH 7.4, 140 mM NaCl, and 5 mM KCl supplemented with 2 mM $CaCl_2$ and 2 mM $MgCl_2$) were placed on ice and incubated with purified and Dy647-labeled CyaA or $HlyA_{1–563}/CyaA_{860–1706}$ hybrids for 15 min at 4 °C. Finally, the cells were washed and resuspended in cold HBSS buffer, and the amounts of fluorescently labeled proteins bound to the surface of cells were determined by flow cytometry.

2.7. Determination of hemolytic activity

Hemolytic activity was measured in TNC buffer by determining the hemoglobin release (A_{541} nm) upon toxin incubation with washed sheep erythrocytes (LabMediaServis, Jaromer, Czech Republic) (5×10^8/ml) as previously described [71].

2.8. Competition assay in CR3-expressing CHO cells

CHO-CR3 cells (10^5 in 200 μl) were incubated with the tested competitor proteins (at concentrations ranging from 0 to 175 nM) in HEPES-buffered salt solution (10 mM HEPES pH 7.4, 140 mM NaCl, 5 mM KCl) supplemented with 2 mM $CaCl_2$, 2 mM $MgCl_2$, 1 % (*w/v*) glucose, and 1 % (*v*/v) FCS for 15 min on ice. Dy647-labeled CyaA-AC$^-$ was then added to the cells to a final concentration of 5.6 nM, and the samples were incubated on ice for 30 min. The binding of Dy647-labeled CyaA-AC$^-$ to cells was then analyzed by flow cytometry (FACS LSR II, BD Biosciences, USA) in the presence of 1 μg/ml of Hoechst 33258 vital dye. Data were analyzed using the FlowJo software (Tree Star, USA) and appropriate gating was used to exclude cell aggregates. Binding data were deduced from the mean fluorescence intensities (MFIs) of the cell-associated Dy647-labeled CyaA-AC$^-$, where the MFI of the cell-bound Dy647-labeled CyaA-AC$^-$ in the absence of a competitor protein was taken as 100 %.

2.9. Lipid bilayers

Measurements on planar lipid bilayers were performed in Teflon cells as described previously [14]. The membrane was formed by the painting method using L-α-phosphatidylcholine, (asolectin, type II-S, Sigma-Aldrich) in n-decane–butanol (9:1, vol/vol). Both compartments contained 150 mM KCl, 10 mM Tris-HCl pH 7.4, and 2 mM $CaCl_2$, and the temperature was 25 °C. Membrane current was recorded with Ag/AgCl electrodes (Theta) with salt bridges (applied voltage −50 mV), amplified with LCA-200-100G and LCA-200-10G amplifiers (Femto, Berlin, Germany), and digitized with a LabQuest Mini A/D converter (Vernier, Beaverton, OR). For lifetime determination, dwell times were determined using QuB software with 100 Hz low-pass filter. Kernel density estimation was fitted with an exponential function using Gnuplot software.

2.10. Cell viability assay

Cell viability was determined in D-MEM medium using the WST-1 assay kit (Roche, Basel, Suisse).

2.11. Liquid chromatography-mass spectrometry analysis (LC FT-ICR MS)

The MS analysis was performed using a solariX XR FTMS instrument equipped with a 15 T superconducting magnet and a Dual II ESI/MALDI ion source (Bruker Daltonics, Billerica, USA), as described earlier [72]. Briefly, proteins were dissolved in 50 mM ammonium bicarbonate buffer (pH 8.2) to reach 4 M concentration of urea and digested in-solution using trypsin (Promega (Madison, WI), modified sequencing grade) at a trypsin/protein ratio of 1:50 for 6 h at 30 °C. A second addition of trypsin followed to reach a final trypsin/protein ratio of 1:25, and the reaction continued for another 6 h at 30 °C. The resulting peptides were adjusted to a concentration of 0.1 mg/ml by 0.1 % TFA, and 5 μl of the samples were injected into the LC–MS system. The LC separation was performed using a desalting column (ZORBAX C18 SB-300, 0.1 3 2 mm) at a flow rate of 40 ml/min (Shimadzu, Kyoto, Japan) of 0.1 % formic acid (FA) and a separation column (ZORBAX C18 SB300, 0.23150 mm) at a flow rate of 10 ml/min (Agilent 1200, Santa Clara, CA) of water/acetonitrile (MeCN) (Merck, Darmstadt, Germany) gradient: 0–1 min, 0.2 % FA, 5 % MeCN; 5 min, 0.2 % FA, 10 % MeCN; 35 min, 0.2 % FA, 50 % MeCN; 40 min, 0.2 % FA, 95 % MeCN; 40–45 min, 0.2 % FA, 95 % MeCN. A capillary column was directly connected to a mass analyzer. Spectra were processed using the Data Analysis 4.4 software package (Bruker Daltonics) and the extracted data were searched either against the FASTA of an intact toxin molecule (CyaA, UniProtKB P0DKX7; HlyA, UniProtKB: P08715) or its sequence modified in accordance with corresponding mutation using Linx software (RRID: SCR_018657). The acylation status of proteins was determined by comparing the relative intensity ratios between all peptides containing fatty acid modifications of corresponding lysine residues at specific positions (CyaA: 860,983; HlyA: 564,690) and their unmodified counterparts [69].

2.12. Structure prediction

AlphaFold 2 [73] was used to predict the structure of proteins using standard settings.

2.13. Statistical analysis

Results were expressed as arithmetic mean ± standard deviation (SD) of the mean. Unpaired Student's *t*-test or one-way ANOVA was used to calculate statistical significance (GraphPad Prism 9.1.1; GraphPad Software, La Jolla, CA). Significant differences are indicated by asterisks ($*p < 0.05$;$**p < 0.01$; $***p < 0.001$; $****p < 0.0001$).

3. Results

3.1. A mono-C16-acylated $HlyA_{1–563}/CyaA_{860–1706}$ chimera is as hemolytic and cytotoxic as the C14-bi-acylated native HlyA

To test the ability of the RTX domain of CyaA to support the formation of cytolytic pores by the pore-forming domain of HlyA, we generated CyaC- and HlyC- activated $HlyA_{1–563}/CyaA_{860–1706}$ hybrid molecules (Fig. 1A, B, and C). The $HlyA_{1–563}/CyaA_{860–1706}$ chimera was produced in *E. coli* cells in the presence of either the CyaA-activating CyaC acyltransferase, or together with the HlyA-activating HlyC acyltransferase, and the acylation status of the purified chimeras (Fig. 1B) was determined by LC FT-ICR mass spectrometry. As shown in Table 1, both CyaC and HlyC acyltransferases recognized only poorly the $Lys564_{HlyA}/Lys860_{CyaA}$ residue within the chimeric acylation site, flanked N-terminally by the HlyA sequence preceding the Lys564 and C-terminally by the CyaA sequence following the Lys860 residue (Fig. 1D). Only 14 % of the $Lys564_{HlyA}/Lys860_{CyaA}$ residues of the $HlyA_{1–563}/CyaA_{860–1706}$ chimera was acylated by CyaC with C16 acyl chains, namely the palmitoyl (C16:0) and palmitoleyl (C16:1) residues. The HlyC acyltransferase then failed to acylate the $Lys564_{HlyA}/Lys860_{CyaA}$ residue of the chimera at all. However, both the cognate acyltransferase CyaC, as well as the heterologous acyltransferase HlyC, recognized quite efficiently the second CyaA acylation site of the $HlyA_{1–563}/CyaA_{860–1706}$ chimera at the K983 residue (CyaA sequence numbering). 92 % of the hybrid molecules were modified by CyaC at Lys983 by C16:0, C16:1 or

Table 1
Acylation status of the CyaA, HlyA and $HlyA_{1–563}/CyaA_{860–1706}$ hybrids.

Protein[a]	Modification	Lys860[b]	Lys983[b]
CyaA	Non-modified	4	3
(CyaC-activated)	C16:0	36	35
	C16:1	53	54
	C18:1	7	8
		Lys564[b]	Lys690[b]
HlyA	Non-modified	0	0
(HlyC-activated)	C14:0	47	72
	C14:0-OH	52	27
		Lys860[b]	Lys983[b]
$HlyA_{1-563}/$ $CyaA_{860–1706}$	Non-modified	86	8
	C16:0	2	39
(CyaC-activated)	C16:1	12	47
	C18:1	0	3
		Lys860[b]	Lys983[b]
$HlyA_{1-563}/$ $CyaA_{860–1706}$	Non-modified	99	42
	C14:0	1	52
(HlyC-activated)	C14:0-OH	0	6

[a] Proteins were produced in *E. coli* XL-1 cells and purified to homogeneity as described in Materials and methods.

[b] Percentage distribution of fatty acid modification of the ε-amino groups of Lys860, Lys983, Lys564 and Lys690. Average values are derived from determinations performed with two different toxin preparations. The numbering of the acylated lysine residues is based on the full-length sequence of CyaA and HlyA. The remaining lysine residues to 100 % are acylated by small amounts of C12:0, C12:0-OH, C14:1 and C16:1-OH.

some C18:1 acyl chains, as in the intact CyaA (Table 1). By difference, HlyC acyltransferase modified 58 % of the chimeric molecules on Lys983 by a mixture of fourteen carbon-long myristoyl (C14:0) and hydroxymyristoyl (C14:0-OH) acyl residues. These data show that both CyaC and HlyC acyltransferases recognized rather poorly the hybrid acylation site motif surrounding the hybrid $Lys564_{HlyA}/Lys860_{CyaA}$ site in the $HlyA_{1–563}/CyaA_{860–1706}$ chimera. This indicates that both toxin activating acyltransferases need to recognize the corresponding cognate acylation site sequences/structures located both N-terminally and C-terminally of the modified Lys564 or Lys860 residues, respectively. The stringency for the second acylation site was lower and the heterologous acyltransferase HlyC modified 58 % of the Lys983 residue of CyaA while using as substrate exclusively the C14 chain-loaded acyl-ACP. These results further confirm our previous observation [39,69] that the RTX toxin activating acyltransferases CyaC and HlyC use highly selectively the acyl-ACP substrates loaded with acyl chains of differing lengths (*e.g.* C16 for CyaC and C14 for HlyC, respectively).

To assess the impact of the length of attached acyl chains on the capacity of the $HlyA_{1–563}/CyaA_{860–1706}$ chimera to bind and permeabilize cells, we first used sheep erythrocytes as model target cells devoid of β_2 integrin receptors. As shown in Fig. 2A when erythrocyte binding capacity of the near-completely C16-mono-acylated (CyaC-activated) $HlyA_{1–563}/CyaA_{860–1706}$ chimera was taken as 100 %, the partially (*e.g.* 58 %) C14-mono-acylated $HlyA_{1–563}/CyaA_{860–1706}$ toxin exhibited 45 % capacity to bind erythrocytes. Hence, the reduced cell binding capacity of the chimeric toxin correlated well with the reduced extent of C14 acyl modification of the Lys983 residue. However, only the Lys983-attached C16 acyls and not the linked C14 acyls, effectively conferred a pore-forming capacity on the chimera (Fig. 2B). Under the used conditions of 20 min of incubation with the toxins at equal concentrations, where the C16-acylated CyaA toxin did not trigger any erythrocyte lysis (Supplementary Fig. 3A), the C16-mono-acylated $HlyA_{1–563}/CyaA_{860–1706}$ hybrid exhibited an as high hemolytic activity on sheep erythrocytes as the intact C14-bi-acylated HlyA (CL_{50} 0.4 nM). In contrast, the incompletely mono-C14-acylated $HlyA_{1–563}/CyaA_{860–1706}$ hybrid exhibited a disproportionately low hemolytic potency over a wide range of protein concentrations ($CL_{50} > > 5$ nM). In fact, the specific hemolytic activity of the C14-acylated $HlyA_{1–563}/CyaA_{860–1706}$ hybrid was much lower than expected, given its rather high erythrocyte binding capacity (*e.g.* 45 %) and its high extent of C14 mono-acylation (*e.g.* 58 %).

We thus set out to ascertain whether the modification by C14 acyls, or the presence of ~40 % of non-acylated chimeric molecules in the toxin preparation, accounted for the very low specific hemolytic activity of the C14-acylated chimera. To this end, we reduced the fraction of acylated molecules to a comparable level also in the preparation of the C16-acylated chimeric toxin (acylated to ~90 % on Lys983), admixing it in a molar ratio of 3:1 with non-acylated chimeric molecules produced in the absence of CyaC. Nevertheless, such preparation containing ~65 % of C16-acylated toxin molecules still exhibited a much higher specific hemolytic activity (CL_{50} 0.9 nM) than the C14-activated hybrid toxin preparation ($CL_{50} > > 5$ nM, Fig. 2B). It can thus be concluded that modification of the Lys983 residue by C14 acyls activated the chimeric toxin very poorly. This reveals a very strict requirement for a functional match of the length (C16) of the attached acyl chain with the structure of the RTX moiety of CyaA, which decisively rules the insertion of the adjacent pore-forming moiety into cell membrane.

To corroborate this observation, we examined the ability of the differently acylated $HlyA_{1–563}/CyaA_{860–1706}$ chimeras to bind and lyze nucleated Chinese hamster ovary cells (CHO). As shown in Fig. 2C, the partially C14-acylated $HlyA_{1–563}/CyaA_{860–1706}$ chimera exhibited 71 % of the capacity of the C16-acylated chimera to bind CHO cells. As on erythrocytes, the C16-mono-acylated $HlyA_{1–563}/CyaA_{860–1706}$ chimera exhibited an equal cytotoxic potency on CHO cells as the intact bi-acylated HlyA (CV_{50} ~ 6 nM). In contrast, the C14-mono-acylated $HlyA_{1–563}/CyaA_{860–1706}$ chimera exhibited more than an order of magnitude lower cytotoxicity over a wide range of protein concentrations (CV_{50} 80 nM, Fig. 2D), whereas fully pore-forming and enzymatically inactive CyaA-AC^- toxoid, devoid of its cytotoxic ATP-depleting activity [8], was not cytotoxic against CHO cells at all (Supplementary Fig. 3B). Hence, only the C16 acyl modification of Lys983 of the $HlyA_{1–563}/CyaA_{860–1706}$ chimera was sufficient for near-identical cytotoxic potency towards CHO cells, as that observed for intact C14-bi-acylated HlyA. The latter was, however, much more toxic to cells expressing the LFA-1 (CD11a/CD18) receptor of HlyA (Supplementary Fig. 3, panel D).

3.2. *The C16-mono-acylated $HlyA_{1–563}/CyaA_{860–1706}$ chimera forms HlyA-like pores*

To analyze the molecular basis of the cell-permeabilizing capacity of the $HlyA_{1–563}/CyaA_{860–1706}$ chimera, we determined the overall membrane activity and the distribution of conductance and lifetimes of pores formed by the C14- and C16-acylated hybrids in artificial planar lipid bilayer membranes. The 20 nM intact C14-bi-acylated HlyA and the C16-activated mono-acylated $HlyA_{1–563}/CyaA_{860–1706}$ hybrid produced a similarly steep time-dependent increase in conductance across the asolectin planar lipid bilayer with applied −50 mV potential (Fig. 3A). In contrast, equal amounts of the C14-acylated $HlyA_{1–563}/CyaA_{860–1706}$ hybrid reproducibly caused much lower increase of conductance across the lipid membrane (Fig. 3A). Nevertheless, under single pore resolution conditions (1 nM toxin) the few pores formed by the C14-acylated chimera exhibited similar size (conductance distribution) as the much more frequently formed pores of the C16-acylated chimera and the native C14-bi-acylated HlyA toxin (Fig. 3B and C). In 150 mM KCl and 2 mM $CaCl_2$ at pH 7.4, the intact HlyA and the C16- and C-14-activated $HlyA_{1–563}/CyaA_{860–1706}$ hybrids formed a range of conductance units, with the most frequent pore conductance being ~500 pS (Fig. 3C). However, all three proteins formed also smaller conductance units (<400 pS) that possibly reflect the stoichiometric intermediates arising during the pore oligomer association-dissociation process. Moreover, the smaller conductance units were more frequently observed with the incompletely C14-mono-acylated chimeric protein (Fig. 3C), possibly reflecting its slower kinetics of oligomerization into the main conductance unit (highest order oligomer), or its faster dissociation into lower

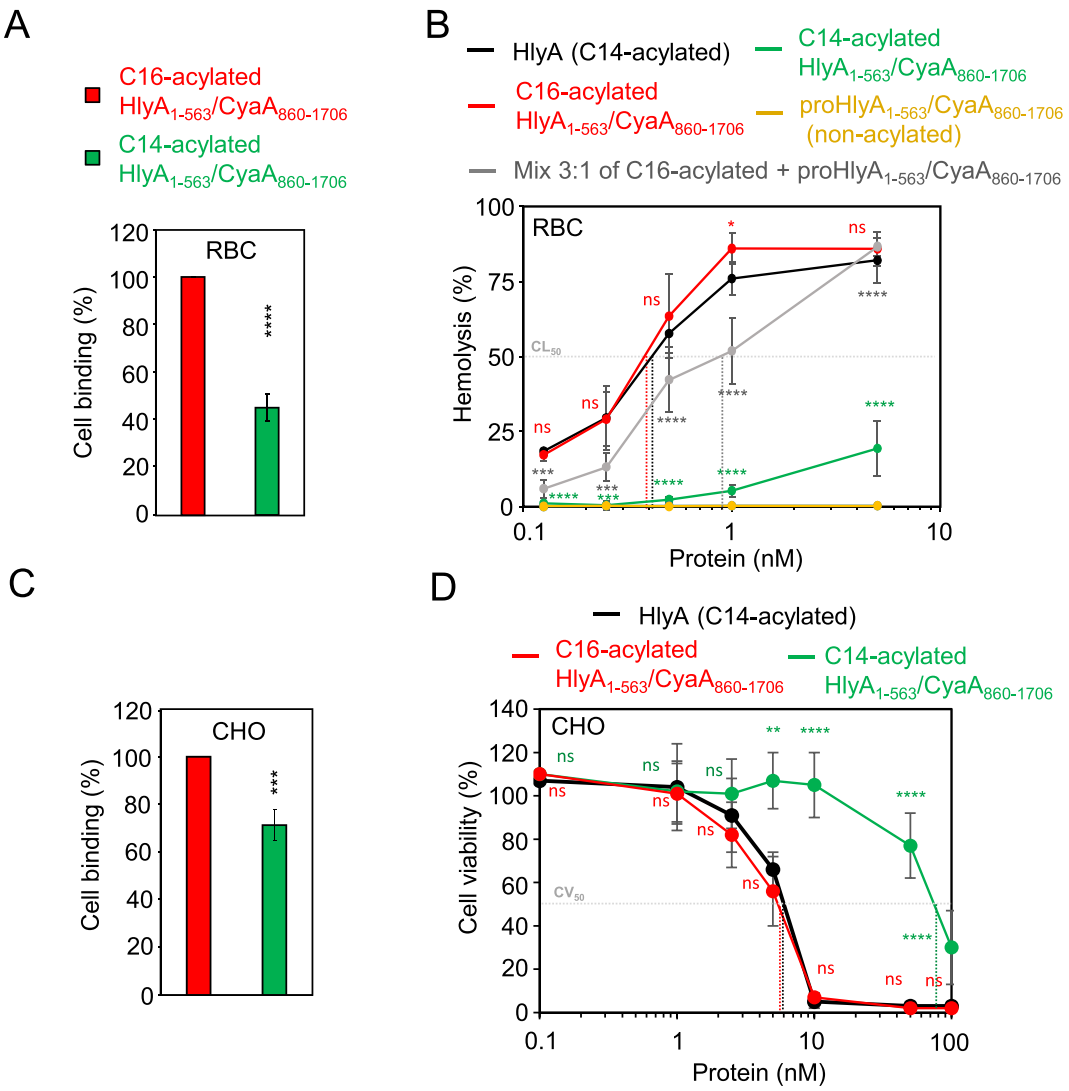

Fig. 2. The C16-mono-acylated $HlyA_{1–563}/CyaA_{860–1706}$ chimera and the intact C14-bi-acylated HlyA exhibit an equal specific cytolytic activity on cells lacking β_2 integrins. (A) Both the C16-acylated and the C14-acylated hybrids bind well to sheep erythrocytes. Washed erythrocytes (5×10^5/200 μl) in TNC buffer (Tris 50 mM, NaCl 150 mM, $CaCl_2$ 2 mM, pH 7.4) were supplemented with 100 mM polyethylene glycol 1500 (PEG 1500) that inhibits toxin-mediated cell lysis and incubated with purified and Dy647-labeled $HlyA_{1–563}/CyaA_{860–1706}$ hybrids (15 nM) for 15 min at 4 °C. The erythrocytes were washed, resuspended in cold TNC-PEG 1500 buffer and the amounts of fluorescently labeled proteins bound to the surface of erythrocytes were determined by flow cytometry. The amount of the bound C16-acylated hybrid was taken as 100 %. Mean values ± standard deviations of two independent determinations are shown. (B) The C14-mono-acylated hybrid exhibits very low hemolytic activity, whereas the C16-mono-acylated hybrid possesses an equal specific cytolytic capacity as the intact C14-bi-acylated HlyA. Sheep erythrocytes (5×10^8/ml) were incubated at 37 °C in TNC buffer with the purified proteins at indicated concentrations and extent of hemolysis was determined after 20 min as the amount of released hemoglobin (A_{541nm}). Complete lysis of erythrocytes was expressed as 100 %. Each point represents the mean ± SD of three independent determinations performed in duplicate with two independent protein preparations. CL_{50} was determined as the concentration of toxin causing 50 % hemoglobin release from 5×10^8/ml sheep erythrocytes after 20 min of incubation at 37 °C in TNC buffer. (C) The C16- and the C14-acylated hybrids bind comparably well to CHO cells that lack β_2 integrin receptors. CHO cells (10^5/100 μl) in HBSS buffer (HEPES-buffered saline; 10 mM HEPES, 140 mM NaCl, and 5 mM KCl supplemented with 2 mM $CaCl_2$ and 2 mM $MgCl_2$, pH 7.4) were incubated on ice with 5 nM chimeras labeled with Dyomics 647 for 15 min. Upon a wash in cold HBSS buffer, the amount of cell bound protein was determined by flow cytometry, with the binding capacity of the C16-acylated hybrid taken as 100 %. Mean values ± standard deviations of two independent determinations are shown. (D) The C14-mono-acylated hybrid exhibits very low cytotoxic activity, whereas the C16-mono-acylated hybrid possesses as high specific cytotoxic capacity as the intact HlyA. Viability of CHO cells (1.5×10^5/well) treated with hybrids or intact HlyA was determined as the ability of mitochondrial dehydrogenases to reduce the tetrazolium salt WST-1 to its formazan product after 2 h of exposure to the toxin at 37 °C. Each point represents the mean ± SD of three independent determinations performed in triplicate with two independent protein preparations. CV_{50}; toxin concentration required for 50 % cell viability (1.5×10^5 cells) after 2 h of incubation at 37 °C in D-MEM medium. (A, C) Statistical significance was determined using the unpaired Student's *t*-test. ****$p < 0.0001$; ***$p < 0.001$. (B, D) The statistical significance of differences HlyA *vs.* CyaC-activated chimera and HlyA *vs.* HlyC-activated chimera was determined using one-way ANOVA (ns, no significant, $p > 0.05$; *$p < 0.05$; **$p < 0.01$; ***p < 0.001; ****p < 0.0001). Statistical significance of C14-acylated chimera *vs.* mix (3:1) was determined using the unpaired Student's t-test (gray asterixs, ***p < 0.001; ****p < 0.0001).

order oligomers. Indeed, a reduced stability and accelerated dissociation of the main pore unit formed much less frequently by the C14-activated chimera would also be suggested by its shorter mean lifetime (1198 ± 52 ms) compared to pores formed by the C16-mono-acylated hybrid (1699 ± 113 ms, Fig. 3D). As expected from the published pore properties of CyaA, and consistent with its low hemolytic potency [69], intact CyaA formed much smaller single pore units than HlyA with a mean conductance of only 10.3 pS (Supplementary Fig. 4).

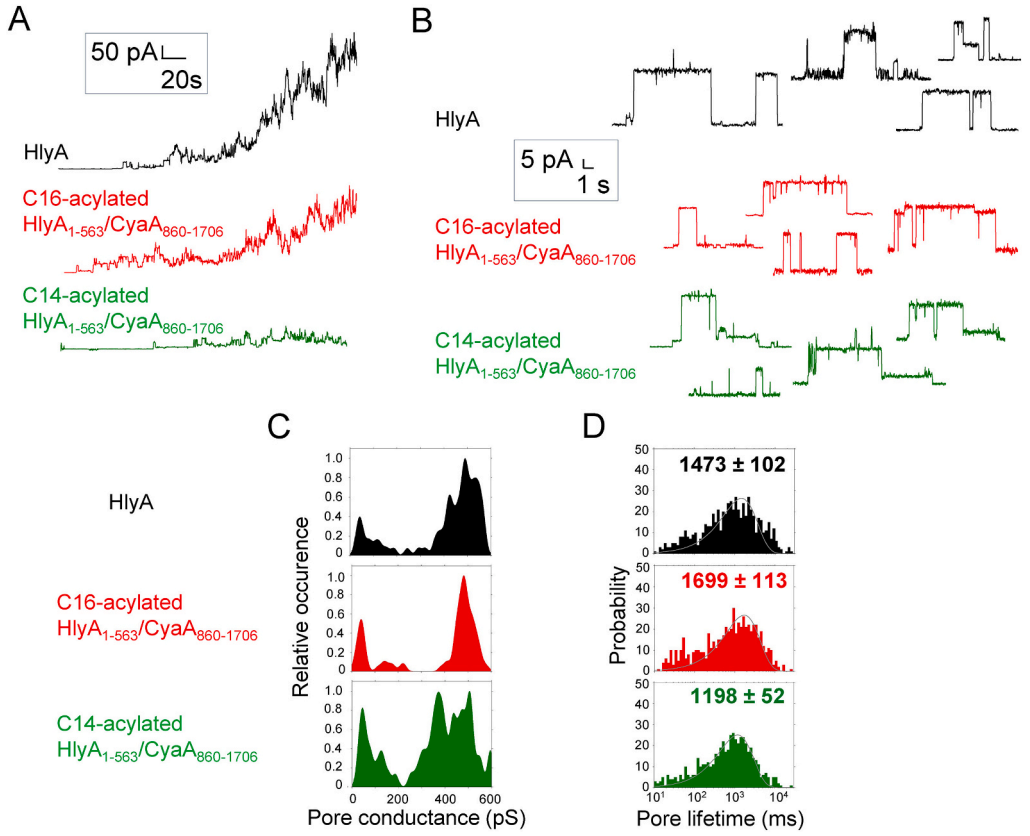

Fig. 3. The chain length of the activating acyls affects the stability of the HlyA-like pores formed by the $HlyA_{1–563}/CyaA_{860–1706}$ chimera. (A) The C14-activated hybrid exhibits very low overall membrane activity, whereas the C16-activated hybrid is endowed with as high membrane permeabilization activity as the intact C14-bi-acylated HlyA toxin. Overall membrane activity of intact HlyA or of the differently acylated hybrids was determined on planar asolectin/decane:butanol (9:1) membranes bathing in 150 mM KCl, 10 mM Tris-HCl (pH 7.4), 2 mM $CaCl_2$ at an applied potential of −50 mV at 25 °C. Toxin concentration was 20 nM. (B) The differently acylated toxin hybrids form HlyA-like membrane pores. Single pore recordings on asolectin membranes exposed to 1 nM purified HlyA or the C16- or C14-acylated $HlyA_{1–563}/CyaA_{860–1706}$ proteins were recorded under the same conditions as in (A). (C) The C14-mono-acylated hybrid form more frequently smaller conductance units than C16-mono-acylated hybrid or the intact C14-bi-acylated HlyA toxin. Kernel density estimation of single-pore conductance of HlyA and the $HlyA_{1–563}/CyaA_{860–1706}$ chimeras (1 nM) calculated from single-pore recordings (500 events) acquired on asolectin membranes under conditions described in (A). (D) The C14-activated hybrid forms pores with shorter lifetime than the C16-activated hybrid, or the intact C14-bi-acylated HlyA toxin. Asolectin membranes were exposed to 1 nM HlyA or $HlyA_{1–563}/CyaA_{860–1706}$ hybrids under the conditions described in (A) and 500 individual pore opening and closing events were plotted as distribution of recorded pore lifetimes. Mean pore lifetimes ± standard deviations are shown.

3.3. Both C16-mono-acylated and C14-mono-acylated HlyA/CyaA chimeras bind CR3 but only the C16-acylated chimera is highly cytotoxic to CR3-expressing cells

The $HlyA_{1–563}/CyaA_{860–1706}$ hybrid possesses an intact CD11b-binding site within the RTX domain, which comprises the linker regions between RTX blocks I and II and blocks II and III, respectively [6,32,52]. Therefore, we tested if the interaction with CR3 would alleviate the functional mismatch of the attached C14 acyl with the RTX domain of CyaA and enable the hybrid toxin to penetrate cell membrane and form pores. As verified for the C16-mono-acylated protein, the $HlyA_{1–563}/CyaA_{860–1706}$ hybrid effectively bound CR3 and its interaction with the CR3-expressing CHO cells (CHO-CR3) was largely inhibited by the anti-CD11b monoclonal antibody M1/70 (Fig. 4A), which engages the same epitope on CD11b as CyaA [6]. Both the C16-mono-acylated, as well as the incompletely C14-mono-acylated $HlyA_{1–563}/CyaA_{860–1706}$ hybrid, were able to outcompete the Dyomics 647-labeled CyaA-AC^{-} toxoid (CyaA-AC^{-} Dy647) from binding to the CD11b subunit of CR3 expressed on CHO-CR3 cells (Fig. 4B). Moreover, the C16-mono-acylated $HlyA_{1–563}/CyaA_{860–1706}$ chimera competed as efficiently for CR3 binding as the intact doubly C16-acylated CyaA. The incompletely C14-mono-acylated $HlyA_{1–563}/CyaA_{860–1706}$ chimera competed about two-fold less efficiently for CR3 binding, proportionately to the extent of its C14 mono-acylation (58 %). In contrast, the HlyA toxin that binds the CD18 subunit of CR3 did not compete for CR3 binding with CyaA-AC^{-} at all, revealing that HlyA binding to CD18 does not sterically obturate the CyaA binding site on the CD11b subunit of the CD11b/CD18 heterodimer that forms CR3 (Fig. 4B). The efficient binding of the C16-acylated chimera to CR3-expressing CHO cells then resulted in three- to fivefold increase of the specific cytotoxic potency of the chimera on CR3-CHO cells as compared to mock-transfected CHO cells devoid of CR3 (Fig. 4C). However, the rather efficient interaction with CR3 (Fig. 4D) still did not rescue the functional defect of the C14-mono-acylated chimera that exhibited a disproportionately reduced, about 10-fold lower cytotoxic potency on CHO-CR3 cells than the C16 mono-acylated chimera (Fig. 4E). Hence, positioning of the chimera towards the plane of the cellular membrane by interaction with the CR3 receptor did not override the functional mismatch of the K983-linked C14 myristoyl chains with the RTX domain structure and did not enable an efficient insertion of the cytotoxic pore-forming segments of the hybrid toxin into the cell membrane.

4. Discussion

We show that a fusion of the large RTX segment of CyaA with the hydrophobic pore-forming module of HlyA can yield a fully functional RTX cytolysin chimera that forms HlyA-like membrane pores. Intriguingly, the capacity of this $HlyA_{1–563}/CyaA_{860–1706}$ hybrid toxin to insert

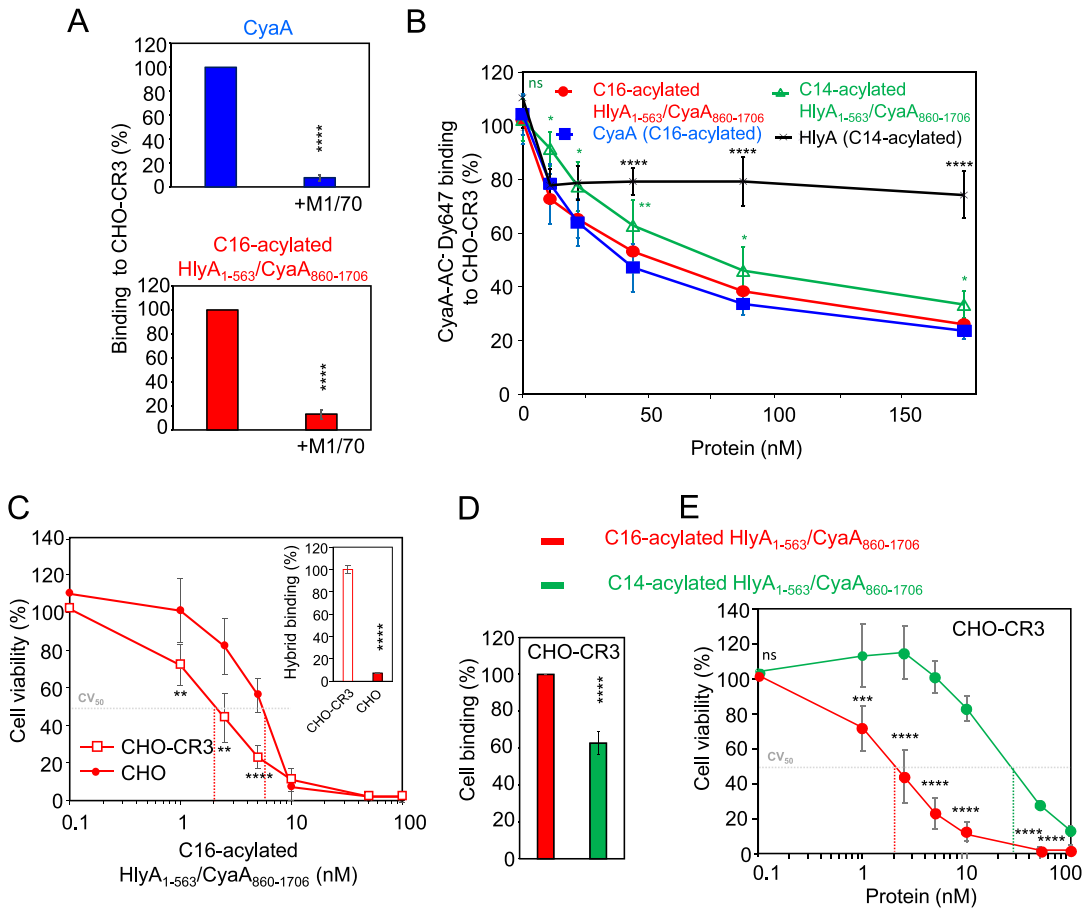

Fig. 4. The chain length of the activating acyl determines the capacity of the CR3-bound $HlyA_{1–563}/CyaA_{860–1706}$ chimera to penetrate cell membrane and form cytotoxic pores. (A) Binding of the hybrid to the CR3 receptor is inhibited by the M1/70 antibody that blocks the CyaA binding site on the CD11b subunit of the β_2 integrin. CHO-CR3 transfectants (3×10^5) in HBSS buffer were pre-incubated with 5 μg/ml of the CD11b-specific monoclonal antibody M1/70 for 20 min on ice before addition of 5 nM CyaA-Dy647 toxin or of 5 nM C16-mono-acylated $HlyA_{1–563}/CyaA_{860–1706}$-Dy647 hybrid for 15 min. Cells were washed in HBSS to remove unbound proteins and the amount of bound Dy647-labeled toxin was determined by FACS analysis. The amount of toxin bound in the absence of the M1/70 mAb was taken as 100 % binding. Means ± standard deviation of three independent determinations are shown. The statistical significance was determined using the unpaired Student's t-test. ****$p < 0.0001$. (B) The mono-C14-acylated hybrid competes for CR3 binding with CyaA-Dy647, albeit less efficiently than the mono-C16-acylated hybrid. Stably transfected CHO-CR3 cells were pre-incubated with CyaA, HlyA, or the hybrid proteins at indicated concentrations on ice for 15 min and CyaA-AC^- Dy647 (5.6 nM) was added for another 30 min of incubation on ice. The amount of CyaA-AC^- Dy647 bound to cell surface was determined by flow cytometry. Results are expressed as the percentage of CyaA-AC^- Dy647 bound in the presence of the indicated competitors. Results are representative of three independent experiments performed in duplicate. The statistical significance of differences CyaA *vs.* HlyC-activated chimera and CyaA *vs.* HlyA was determined using one-way ANOVA (ns, no significant, $p > 0.05$; *$p < 0.05$; ****$p < 0.0001$). No significant difference in competition for CR3 binding was observed for CyaA *vs.* CyaC-activated chimera ($p > 0.05$ in all tested concentrations). (C) CR3 expression increases the susceptibility of CHO cells to cytotoxic action of the C16-mono-acylated hybrid. CR3-expressing CHO transfectants (CHO-CR3, 1.5×10^5/well), or mock-transfected CHO cells (CHO, 1.5×10^5/well), were exposed to indicated concentration of the hybrid for 2 h at 37 °C and their viability was determined as described in legend to Fig. 2D. Each point represents the mean ± SD of three independent determinations performed in triplicate with two independent protein preparations. (Insert) CHO-CR3 or CHO cells (2×10^5/200 μl) in HBSS buffer were incubated for 15 min on ice with 5 nM mono-palmitoylated hybrid, washed in HBSS and cell binding was determined by FACS. Hybrid binding to CHO-CR3 cells was taken as 100 %. The means ± standard deviations of two independent determinations are shown. The statistical significance was determined using the unpaired Student's t-test. **$p < 0.01$; ****$p < 0.0001$. (D, E) Despite comparable capacity to bind CR3-expresing cells, the C14-mono-acylated hybrid exhibits lower specific cytotoxic activity on CR3-expressing CHO cells than the C16-mono-acylated hybrid. (D) CHO-CR3 cells (10^5/100 μl) in HBSS were incubated on ice with chimeras (5 nM) labeled with Dyomics 647 for 5 min and washed in cold HBSS buffer. The cell binding capacity of the hybrids was determined by flow cytometry. The binding capacity of the C16-activated hybrid was taken as 100 % and average values ± standard deviations of two independent determinations are given. The statistical significance was determined using the unpaired Student's t-test. ****$p < 0.0001$. (E) Cell viability of CHO cells transfected with CR3 (CHO-CR3, 1.5×10^5/well), treated with $HlyA_{1–563}/CyaA_{860–1706}$ hybrids was determined by WST-1 after 2 h of exposure to the toxin at 37 °C. Each point represents the mean ± SD of three independent determinations performed in triplicate with two independent protein preparations. The statistical significance was determined using the unpaired Student's t-test. ns, no significant, $p > 0.05$; ***$p < 0.001$; ****$p < 0.0001$). CV_{50}; toxin concentration required for 50 % cell viability (1.5×10^5 cells) after 2 h of incubation at 37 °C in D-MEM medium.

the HlyA pore-forming module into target cell membrane to form HlyA-like pores depended strictly on the acylation of the CyaA RTX module cap by an acyl chain of CyaA-adapted length. Only modification by the sixteen carbon-long (C16) acyls conferred a full HlyA-like pore-forming activity on the $HlyA_{1–563}/CyaA_{860–1706}$ chimera. Modification by only two carbon-shorter C14 acyls conferred a very low specific pore-forming capacity despite of supporting a rather efficient binding of the hybrid toxin to target cell membrane (45 to 71 %, depending on cell type). These results reveal that for the CyaA RTX cap, the match of the length of the attached acyl chain with some particular structure of the acylated segment does decisively rule its capacity to promote a productive membrane insertion of the adjacent pore-forming module.

We observed recently that the requirement for acylation by an adapted acyl chain length was much less stringent for the acylated RTX

domain cap of HlyA. An inverted $CyaA_{1–710}/HlyA_{411–1024}$ toxin hybrid was equally functional in delivery of the CyaA-derived N-terminal AC enzyme into LFA-1-expressing cells irrespective of whether its HlyA-derived RTX domain cap was acylated by CyaC-attached C16 acyls, or by the C14 acyl chains naturally used by the cognate HlyC acyltransferase [39]. Nevertheless, only the C14 acyl modification conferred on the inverted $CyaA_{1–710}/HlyA_{411–1024}$ chimera the capacity to deliver the AC enzyme into erythrocytes that lack the LFA-1 receptor [39]. Hence, the stringency of the requirement for functional modification by an acyl chain of adapted length appears to depend both on the structure of the acylated RTX domain cap and on the target cell membrane. Namely, whether the toxin insertion into target cell membrane is facilitated by an interaction with a specific β_2 integrin receptor (*e.g.* LFA-1). Intriguingly, the non-natural HlyA RTX cap acylation by C16 acyls still conferred an almost full pore-forming activity to the otherwise C14-acylated intact HlyA toxin [69]. Hence, the requirement for activation by an acyl chain of adapted length appears to be less strict for HlyA than for CyaA.

It is stunning that at equal protein concentrations, the here-characterized C16-mono-acylated $HlyA_{1–563}/CyaA_{860–1706}$ hybrid permeabilized the β_2 integrin receptor-free erythrocytes and nucleated mock CHO cells as efficiently as intact HlyA (*c.f.* Fig. 2), as the two proteins differed importantly in size, structure, and acylation status. In this chimera the single long β-roll structure of the CD18-binding RTX domain of HlyA was replaced by the more than twice larger RTX domain of CyaA that consist of 5 β-roll blocks and binds CD11b [5,41]. Nevertheless, in the absence of a β_2 integrin receptor on the cell surface, the length and overall organization/structure of the RTX domain did not matter and both type of RTX domains apparently mediated a comparably efficient toxin binding to target cell surface, presumably through recognition of glycans [76–79].

It has to be noted, that the $HlyA_{1–563}$ portion of the here-used toxin hybrid was linked to the $CyaA_{860–1706}$ moiety through the first acylated lysine residue of HlyA, *e.g.* Lys564, which became the first acylated Lys860 residue of CyaA in the CyaA numbering (*c.f.* Fig. 1D). This junction point was chosen because of the high degree of similarity of the N-terminal sequences that flank the Lys564 and Lys860 residues of HlyA and CyaA (Fig. 5A and Supplementary Fig. 1). These segments form a β-strands of a β hairpin (*c.f.* Fig. 5B) exposing the acylated Lys564/Lys860 residue on its tip [32]. The high pore-forming and cytolytic activity of the $HlyA_{1–563}/CyaA_{860–1706}$ hybrid would then indicate that the α-helical segments of the pore-forming domain likely fold independently of the acylated RTX cap of the RTX domain, as also indicated by the predicted structure (*c.f.* Fig. 1C).

Moreover, the AlphaFold models of HlyA, $CyaA_{751–1706}$ and of the $HlyA_{1–563}/CyaA_{860–1706}$ hybrid (*c.f.* Fig. 1C) predict a highly similar

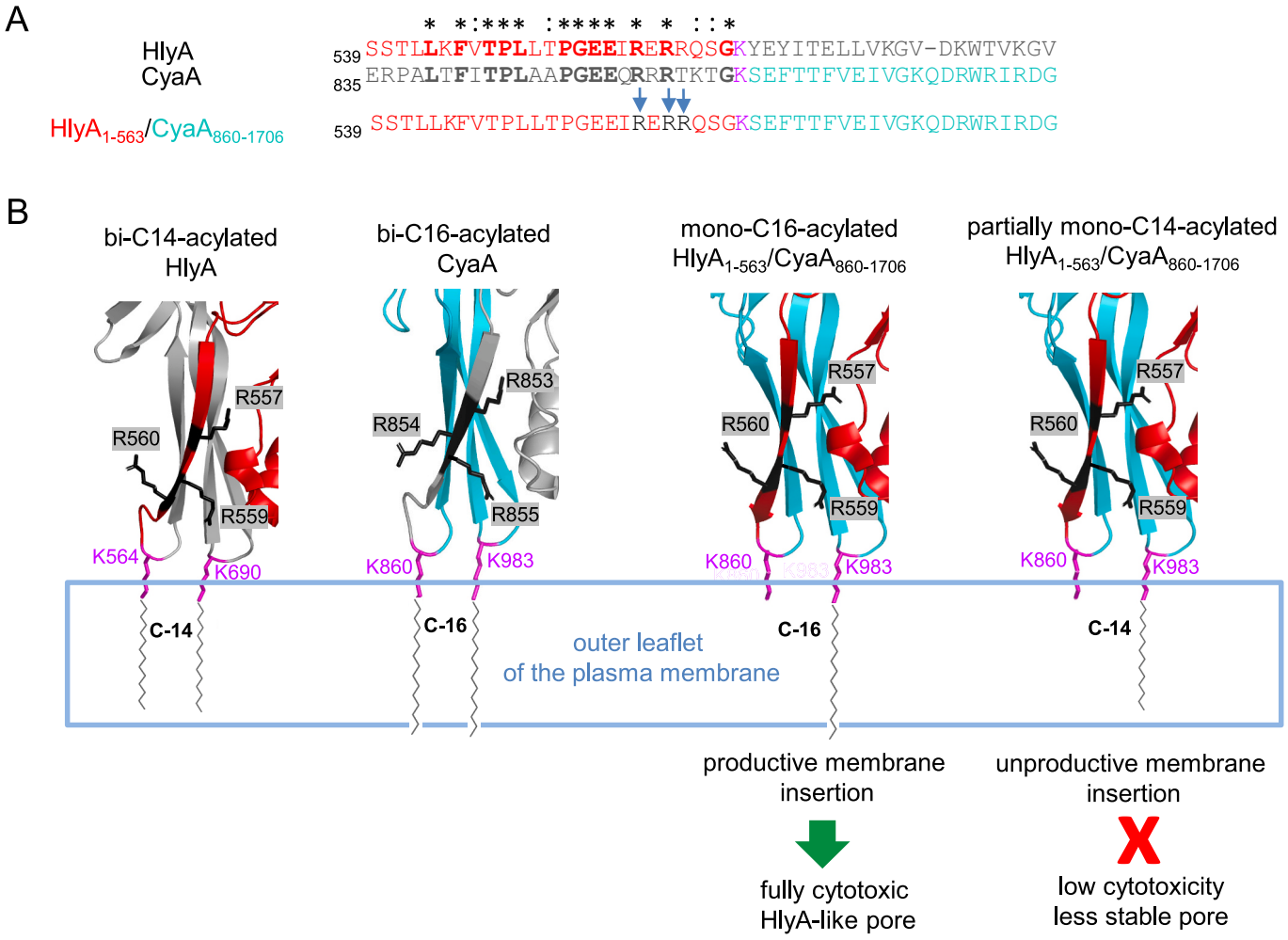

Fig. 5. Schematic representation of the action of the mono-C16-acylated $HlyA_{1–563}/CyaA_{860–1706}$ chimera. (A) The ClustalW sequence alignments of portions of the acylated segments of HlyA and CyaA. HlyA, *Escherichia coli* (NCBI reference sequence WP_000208152.1); CyaA, *Bordetella pertussis* (WP_010929995.1). The acylated lysines are in magenta color. * identity,: strongly similar. The position of arginine residues 557, 559 and 560 of HlyA is highlighted by blue arrows. (B) AlphaFold 2 model of the portions of the acylated segments of HlyA, CyaA fragment 751–1706 (PDB ID: 7USL [32]) and of the differently acylated $HlyA_{1–563}/CyaA_{860–1706}$ hybrids. The parts of HlyA and CyaA that are rendered in gray color absent from the $HlyA_{1–563}/CyaA_{860–1706}$ hybrid. The residues of HlyA and CyaA that are present in the hybrid molecule are labeled in red and cyan colors, respectively. The acylated lysines are in magenta and the arginine residues are in black.

arrangement of the two β hairpins exposing the acylated lysine residues 564/860 and 690/983 of HlyA, CyaA and the HlyA/CyaA chimera at their tips (*c.f.* Fig. 5B). This is compatible with the current model of folding of the RTX domain and of its acylated cap by a series templated mechanism, where at physiological calcium concentrations (~ 2 mM Ca^{2+}) the β-roll blocks fold sequentially, with the folding signal being transferred from the C- to the N-terminus of the molecule [30,32,80–83]. Folding of the Ca^{2+}-loaded RTX domain then drives the folding of its acylated cap and ensures the appropriate orientation of the two β hairpins exposing the acylated lysine residues [32,40], as depicted in Fig. 5B.

Recently, we observed a close and functionally important interaction of the two β hairpins carrying the acylated Lys860 and Lys983 residues of CyaA at their tips [40]. It is noteworthy, that the first β hairpin of both HlyA and CyaA, exposing the Lys564/Lys860 residues, comprises a conserved patch of positively charged arginine residues (Fig. 5A, B), namely R557, R559, and R560 of HlyA, or R853, R854 and R855 of CyaA. It is tempting to speculate that an electrostatic interaction of the positively charged patch of guanidinium groups of these arginine residues with the negatively charged phospholipid headgroups of the outer leaflet of the cellular lipid bilayer membrane may facilitate membrane insertion of the acyl chains linked to the tips of the two interacting β hairpins. This would likely anchor the toxin into cell membrane and bring the adjacent pore-forming domain into close vicinity of membrane surface, thereby facilitating the penetration of the hydrophobic and amphipathic α-helices of the pore-forming domain into the lipid bilayer of cell membrane.

In this respect, it is puzzling that only a modification of the Lys983 residue by C16 acyl chains enables the acylated CyaA RTX cap to support membrane insertion pore-forming domain and formation of functional pores. It remains to be elucidated by structural studies whether the Lys983-linked acyls make any functional contacts with any sort of a 'molecular ruler' structure on the RTX cap of CyaA, which would distinguish between C16 and C14 acyls. It is conceivable that such interaction could confer a functional structure on some toxin segment playing a critical role in membrane penetration of the pore-forming domain. In any case, the here-reported result goes well with our previous observations that mono-palmitoylation on the Lys983 residue of CyaA is necessary and sufficient for productive membrane insertion of CyaA into both erythrocyte and macrophage membranes [50,54].

It is also worth noting that the characteristics of pores formed by the intact C14-bi-acylated HlyA and the C16-mono-acylated $HlyA_{1–563}$/$CyaA_{860–1706}$ chimera were quite similar (*c.f.* Fig. 3). Intriguingly, the distribution pattern of unit conductance occurrence and the distribution of lifetimes of pores formed by the mono-acylated $HlyA_{1–563}$/$CyaA_{860–1706}$ chimera was also modulated by the length of the toxin-attached acyl chains. The incompletely C14-acylated hybrid formed lower conductance units more frequently than the C16-acylated hybrid. Moreover, the conductance units formed by the C14-acylated chimera exhibited a decreased lifetime, suggesting that the C14-acylated chimera formed less stable pores than the C16 mono-acylated chimera (*c.f.* Fig. 3). The increased occurrence of smaller conductance units would then presumably correspond to increased occurrence of lower order oligomers, or pore assembly-disassembly intermediates of the C14-acylated hybrid. Indeed, the mean lifetime of pores formed by the C14-acylated hybrid was importantly decreased compared to the mean lifetime of pores formed by the C16-acylated hybrid (*e.g.* 1198 ± 52 ms *versus* 1699 ± 113 ms). This may reflect a slower kinetics of oligomerization of the C14 mono-acylated chimera into the pore structure, as well as a reduced stability and faster dissociation kinetics of the pores formed by the C14-acylated molecules. The length of the Lys983-linked acyl chain would thus modulate not only the propensity of membrane insertion but also the association-dissociation equilibrium and stability of the $HlyA_{1–563}$/$CyaA_{860–1706}$ hybrid pore.

5. Conclusions

We show here that two functional modules of two different RTX toxins, namely the pore-forming module of α-hemolysin from *Escherichia coli* and the calcium-binding and acylated RTX segment of adenylate cyclase toxin from *Bordetella pertussis* can form a fully functional chimeric pore-forming cytolytic toxin, providing that the used RTX domain is modified by structurally matching acyl chains of adapted length.

CRediT authorship contribution statement

Anna Lepesheva: Visualization, Investigation. **Michaela Grobarcikova:** Visualization, Investigation. **Adriana Osickova:** Supervision, Investigation. **David Jurnecka:** Visualization, Investigation. **Sarka Knoblochova:** Investigation. **Monika Cizkova:** Visualization, Investigation. **Radim Osicka:** Writing – review & editing, Visualization, Investigation. **Peter Sebo:** Writing – review & editing, Funding acquisition. **Jiri Masin:** Writing – original draft, Visualization, Supervision, Project administration, Investigation, Funding acquisition, Formal analysis, Conceptualization.

Declaration of competing interest

The authors declare that they have no known competing financial interests or personal relationships that could have appeared to influence the work reported in this paper.

Data availability

The mass spectrometry proteomics data have been deposited to the ProteomeXchange Consortium [74] *via* the PRIDE [75] partner repository with the data set identifier PXD046160. All data pertinent to this work are contained within this manuscript or available upon request. For requests, please contact: Jiri Masin, masin@biomed.cas.cz.

Acknowledgements

We thank Sona Kozubova, Iva Marsikova, and Oliva Branna for excellent technical help. Monika Cizkova is a doctoral student at the University of Chemistry and Technology. The research infrastructure projects LM2023053 (EATRIS-CZ) and LM2023042 (CIISB) of the Ministry of Education, Youth and Sports of the Czech Republic and grant number 22-15825S (R.O.) from the Czech Science Foundation are gratefully acknowledged. We also acknowledge support from Talking microbes - understanding microbial interactions within One Health framework (CZ.02.01.01/00/22_008/0004597).

Funding sources

This work was supported by the Czech Science Foundation (grant number 22-01558S, J. M. and grant number 19-27630X, P. S.) and the project National Institute of Virology and Bacteriology (Programme EXCELES, ID Project No. LX22NPO5103) Funded by the European Union - Next Generation EU.

Abbreviations

RTX	repeat-in-toxin
AC	adenylate cyclase
CyaA	adenylate cyclase toxin
HlyA	α-hemolysin
CR3	complement receptor 3
LFA-1	lymphocyte function-associated antigen 1
RBC	red blood cells
CHO	chinese hamster ovary cells

liquid chromatography coupled to Fourier transform ion cyclotron resonance mass spectrometry LC FT-ICR MS

Appendix A. Supplementary data

Supplementary data to this article can be found online at https://doi.org/10.1016/j.bbamem.2024.184311.

References

[1] I. Linhartova, L. Bumba, J. Masin, M. Basler, R. Osicka, J. Kamanova, K. Prochazkova, I. Adkins, J. Hejnova-Holubova, L. Sadilkova, J. Morova, P. Sebo, RTX proteins: a highly diverse family secreted by a common mechanism, FEMS Microbiol. Rev. 34 (2010) 1076–1112.

[2] J. Novak, O. Cerny, A. Osickova, I. Linhartova, J. Masin, L. Bumba, P. Sebo, R. Osicka, Structure-function relationships underlying the capacity of bordetella adenylate cyclase toxin to disarm host phagocytes, Toxins 9 (2017).

[3] P. Sebo, R. Osicka, J. Masin, Adenylate cyclase toxin-hemolysin relevance for pertussis vaccines, Expert Rev. Vaccines 13 (2014) 1215–1227.

[4] J. Vojtova, J. Kamanova, P. Sebo, Bordetella adenylate cyclase toxin: a swift saboteur of host defense, Curr. Opin. Microbiol. 9 (2006) 69–75.

[5] P. Guermonprez, N. Khelef, E. Blouin, P. Rieu, P. Ricciardi-Castagnoli, N. Guiso, D. Ladant, C. Leclerc, The adenylate cyclase toxin of Bordetella pertussis binds to target cells via the alpha(M)beta(2) integrin (CD11b/CD18), J. Exp. Med. 193 (2001) 1035–1044.

[6] R. Osicka, A. Osickova, S. Hasan, L. Bumba, J. Cerny, P. Sebo, Bordetella adenylate cyclase toxin is a unique ligand of the integrin complement receptor 3, Elife 4 (2015) e10766.

[7] R. Benz, E. Maier, D. Ladant, A. Ullmann, P. Sebo, Adenylate cyclase toxin (CyaA) of Bordetella pertussis. Evidence for the formation of small ion-permeable channels and comparison with HlyA of Escherichia coli, J. Biol. Chem. 269 (1994) 27231–27239.

[8] M. Basler, J. Masin, R. Osicka, P. Sebo, Pore-forming and enzymatic activities of Bordetella pertussis adenylate cyclase toxin synergize in promoting lysis of monocytes, Infect. Immun. 74 (2006) 2207–2214.

[9] R. Fiser, J. Masin, L. Bumba, E. Pospisilova, C. Fayolle, M. Basler, L. Sadilkova, I. Adkins, J. Kamanova, J. Cerny, I. Konopasek, R. Osicka, C. Leclerc, P. Sebo, Calcium influx rescues adenylate cyclase-hemolysin from rapid cell membrane removal and enables phagocyte permeabilization by toxin pores, PLoS Pathog. 8 (2012) e1002580.

[10] E.L. Hewlett, G.M. Donato, M.C. Gray, Macrophage cytotoxicity produced by adenylate cyclase toxin from Bordetella pertussis: more than just making cyclic AMP!, Mol. Microbiol. 59 (2006) 447–459.

[11] T. Wald, A. Osickova, J. Masin, P.M. Liskova, I. Petry-Podgorska, T. Matousek, P. Sebo, R. Osicka, Transmembrane segments of complement receptor 3 do not participate in cytotoxic activities but determine receptor structure required for action of Bordetella adenylate cyclase toxin, Pathog. Dis. 74 (2016).

[12] T. Wald, I. Petry-Podgorska, R. Fiser, T. Matousek, J. Dedina, R. Osicka, P. Sebo, J. Masin, Quantification of potassium levels in cells treated with Bordetella adenylate cyclase toxin, Anal. Biochem. 450 (2014) 57–62.

[13] I.E. Ehrmann, M.C. Gray, V.M. Gordon, L.S. Gray, E.L. Hewlett, Hemolytic activity of adenylate cyclase toxin from Bordetella pertussis, FEBS Lett. 278 (1991) 79–83.

[14] J. Masin, A. Osickova, A. Sukova, R. Fiser, P. Halada, L. Bumba, I. Linhartova, R. Osicka, P. Sebo, Negatively charged residues of the segment linking the enzyme and cytolysin moieties restrict the membrane-permeabilizing capacity of adenylate cyclase toxin, Sci. Rep. 6 (2016) 29137.

[15] O. Subrini, A.C. Sotomayor-Perez, A. Hessel, J. Spiaczka-Karst, E. Selwa, N. Sapay, R. Veneziano, J. Pansieri, J. Chopineau, D. Ladant, A. Chenal, Characterization of a membrane-active peptide from the Bordetella pertussis CyaA toxin, J. Biol. Chem. 288 (2013) 32585–32598.

[16] A. Sukova, L. Bumba, P. Srb, V. Veverka, O. Stanek, J. Holubova, J. Chmelik, R. Fiser, P. Sebo, J. Masin, Negative charge of the AC-to-Hly linking segment modulates calcium-dependent membrane activities of Bordetella adenylate cyclase toxin, Biochim. Biophys. Acta Biomembr. 1862 (2020) 183310.

[17] A. Voegele, M. Sadi, D.P. O'Brien, P. Gehan, D. Raoux-Barbot, M. Davi, S. Hoos, S. Brule, B. Raynal, P. Weber, A. Mechaly, A. Haouz, N. Rodriguez, P. Vachette, D. Durand, S. Brier, D. Ladant, A. Chenal, A high-affinity calmodulin-binding site in the CyaA toxin translocation domain is essential for invasion of eukaryotic cells, Adv. Sci. 8 (2021) 2003630.

[18] A. Voegele, O. Subrini, N. Sapay, D. Ladant, A. Chenal, Membrane-active properties of an amphitropic peptide from the CyaA toxin translocation region, Toxins 9 (2017).

[19] M. Basler, O. Knapp, J. Masin, R. Fiser, E. Maier, R. Benz, P. Sebo, R. Osicka, Segments crucial for membrane translocation and pore-forming activity of Bordetella adenylate cyclase toxin, J. Biol. Chem. 282 (2007) 12419–12429.

[20] S. Juntapremjit, N. Thamwiriyasati, C. Kurehong, P. Prangkio, L. Shank, B. Powthongchin, C. Angsuthanasombat, Functional importance of the Gly cluster in transmembrane helix 2 of the Bordetella pertussis CyaA-hemolysin: implications for toxin oligomerization and pore formation, Toxicon 106 (2015) 14–19.

[21] J. Masin, J. Roderova, A. Osickova, P. Novak, L. Bumba, R. Fiser, P. Sebo, R. Osicka, The conserved tyrosine residue 940 plays a key structural role in membrane interaction of Bordetella adenylate cyclase toxin, Sci. Rep. 7 (2017) 9330.

[22] A. Osickova, R. Osicka, E. Maier, R. Benz, P. Sebo, An amphipathic alpha-helix including glutamates 509 and 516 is crucial for membrane translocation of adenylate cyclase toxin and modulates formation and cation selectivity of its membrane channels, J. Biol. Chem. 274 (1999) 37644–37650.

[23] J. Roderova, A. Osickova, A. Sukova, G. Mikusova, R. Fiser, P. Sebo, R. Osicka, J. Masin, Residues 529 to 549 participate in membrane penetration and pore-forming activity of the Bordetella adenylate cyclase toxin, Sci. Rep. 9 (2019) 5758.

[24] B. Powthongchin, C. Angsuthanasombat, Effects on haemolytic activity of single proline substitutions in the Bordetella pertussis CyaA pore-forming fragment, Arch. Microbiol. 191 (2009) 1–9.

[25] P. Prangkio, S. Juntapremjit, M. Koehler, P. Hinterdorfer, C. Angsuthanasombat, Contributions of the hydrophobic Helix 2 of the Bordetella pertussis CyaA-hemolysin to membrane permeabilization, Protein Pept. Lett. 25 (2018) 236–243.

[26] E.L. Hewlett, M.C. Gray, I.E. Ehrmann, N.J. Maloney, A.S. Otero, L. Gray, M. Allietta, G. Szabo, A.A. Weiss, E.M. Barry, Characterization of adenylate cyclase toxin from a mutant of Bordetella pertussis defective in the activator gene, cyaC, J. Biol. Chem. 268 (1993) 7842–7848.

[27] M. Hackett, L. Guo, J. Shabanowitz, D.F. Hunt, E.L. Hewlett, Internal lysine palmitoylation in adenylate cyclase toxin from Bordetella pertussis, Science 266 (1994) 433–435.

[28] M. Hackett, C.B. Walker, L. Guo, M.C. Gray, S. Van Cuyk, A. Ullmann, J. Shabanowitz, D.F. Hunt, E.L. Hewlett, P. Sebo, Hemolytic, but not cell-invasive activity, of adenylate cyclase toxin is selectively affected by differential fatty-acylation in Escherichia coli, J. Biol. Chem. 270 (1995) 20250–20253.

[29] P. Sebo, P. Glaser, H. Sakamoto, A. Ullmann, High-level synthesis of active adenylate cyclase toxin of Bordetella pertussis in a reconstructed Escherichia coli system, Gene 104 (1991) 19–24.

[30] L. Bumba, J. Masin, P. Macek, T. Wald, L. Motlova, I. Bibova, N. Klimova, L. Bednarova, V. Veverka, M. Kachala, D.I. Svergun, C. Barinka, P. Sebo, Calcium-driven folding of RTX domain beta-rolls ratchets translocation of RTX proteins through type I secretion ducts, Mol. Cell 62 (2016) 47–62.

[31] J.A. Goldsmith, A.M. DiVenere, J.A. Maynard, J.S. McLellan, Structural basis for antibody binding to adenylate cyclase toxin reveals RTX linkers as neutralization-sensitive epitopes, PLoS Pathog. 17 (2021) e1009920.

[32] J.A. Goldsmith, A.M. DiVenere, J.A. Maynard, J.S. McLellan, Structural basis for non-canonical integrin engagement by Bordetella adenylate cyclase toxin, Cell Rep. 40 (2022) 111196.

[33] T. Rose, P. Sebo, J. Bellalou, D. Ladant, Interaction of calcium with Bordetella pertussis adenylate cyclase toxin. Characterization of multiple calcium-binding sites and calcium-induced conformational changes, J. Biol. Chem. 270 (1995) 26370–26376.

[34] J.P. Issartel, V. Koronakis, C. Hughes, Activation of Escherichia coli prohaemolysin to the mature toxin by acyl carrier protein-dependent fatty acylation, Nature 351 (1991) 759–761.

[35] K.B. Lim, C.R. Walker, L. Guo, S. Pellett, J. Shabanowitz, D.F. Hunt, E.L. Hewlett, A. Ludwig, W. Goebel, R.A. Welch, M. Hackett, Escherichia coli alpha-hemolysin (HlyA) is heterogeneously acylated in vivo with 14-, 15-, and 17-carbon fatty acids, J. Biol. Chem. 275 (2000) 36698–36702.

[36] P. Stanley, V. Koronakis, C. Hughes, Acylation of Escherichia coli hemolysin: a unique protein lipidation mechanism underlying toxin function, Microbiol. Mol. Biol. Rev. 62 (1998) 309–333.

[37] P. Stanley, L.C. Packman, V. Koronakis, C. Hughes, Fatty acylation of two internal lysine residues required for the toxic activity of Escherichia coli hemolysin, Science 266 (1994) 1992–1996.

[38] E.T. Lally, I.R. Kieba, A. Sato, C.L. Green, J. Rosenbloom, J. Korostoff, J.F. Wang, B. J. Shenker, S. Ortlepp, M.K. Robinson, P.C. Billings, RTX toxins recognize a beta2 integrin on the surface of human target cells, J. Biol. Chem. 272 (1997) 30463–30469.

[39] J. Masin, A. Osickova, D. Jurnecka, N. Klimova, H. Khaliq, P. Sebo, R. Osicka, Retargeting from the CR3 to the LFA-1 receptor uncovers the adenylyl cyclase enzyme-translocating segment of Bordetella adenylate cyclase toxin, J. Biol. Chem. 295 (2020) 9349–9365.

[40] A. Osickova, S. Knoblochova, L. Bumba, P. Man, Z. Kalaninova, A. Lepesheva, D. Jurnecka, M. Cizkova, L. Biedermannova, J.A. Goldsmith, J.A. Maynard, J. S. McLellan, R. Osicka, P. Sebo, J. Masin, A conserved tryptophan in the acylated segment of RTX toxins controls their beta(2) integrin-independent cell penetration, J. Biol. Chem. 299 (2023) 104978.

[41] L.C. Ristow, V. Tran, K.J. Schwartz, L. Pankratz, A. Mehle, J.D. Sauer, R.A. Welch, The extracellular domain of the beta2 integrin beta subunit (CD18) is sufficient for Escherichia coli Hemolysin and Aggregatibacter actinomycetemcomitans Leukotoxin cytotoxic activity, mBio 10 (2019).

[42] T.J. Wiles, J.M. Bower, M.J. Redd, M.A. Mulvey, Use of zebrafish to probe the divergent virulence potentials and toxin requirements of extraintestinal pathogenic Escherichia coli, PLoS Pathog. 5 (2009) e1000697.

[43] C. Forestier, R.A. Welch, Nonreciprocal complementation of the hlyC and lktC genes of the Escherichia coli hemolysin and Pasteurella haemolytica leukotoxin determinants, Infect. Immun. 58 (1990) 828–832.

[44] C. Forestier, R.A. Welch, Identification of RTX toxin target cell specificity domains by use of hybrid genes, Infect. Immun. 59 (1991) 4212–4220.

[45] L.C. Ristow, R.A. Welch, Hemolysin of uropathogenic Escherichia coli: a cloak or a dagger? Biochim. Biophys. Acta 1858 (2016) 538–545.

[46] L.C. Ristow, R.A. Welch, RTX toxins ambush immunity's first cellular responders, Toxins 11 (2019).

[47] V. Herlax, L. Bakas, Acyl chains are responsible for the irreversibility in the Escherichia coli alpha-hemolysin binding to membranes, Chem. Phys. Lipids 122 (2003) 185–190.

[48] V. Herlax, S. Mate, O. Rimoldi, L. Bakas, Relevance of fatty acid covalently bound to Escherichia coli alpha-hemolysin and membrane microdomains in the oligomerization process, J. Biol. Chem. 284 (2009) 25199–25210.
[49] R.A. Welch, Pore-forming cytolysins of gram-negative bacteria, Mol. Microbiol. 5 (1991) 521–528.
[50] T. Basar, V. Havlicek, S. Bezouskova, M. Hackett, P. Sebo, Acylation of lysine 983 is sufficient for toxin activity of Bordetella pertussis adenylate cyclase. Substitutions of alanine 140 modulate acylation site selectivity of the toxin acyltransferase CyaC, J. Biol. Chem. 276 (2001) 348–354.
[51] T. Basar, V. Havlicek, S. Bezouskova, P. Halada, M. Hackett, P. Sebo, The conserved lysine 860 in the additional fatty-acylation site of Bordetella pertussis adenylate cyclase is crucial for toxin function independently of its acylation status, J. Biol. Chem. 274 (1999) 10777–10783.
[52] M. El-Azami-El-Idrissi, C. Bauche, J. Loucka, R. Osicka, P. Sebo, D. Ladant, C. Leclerc, Interaction of Bordetella pertussis adenylate cyclase with CD11b/CD18: role of toxin acylation and identification of the main integrin interaction domain, J. Biol. Chem. 278 (2003) 38514–38521.
[53] J.C. Karst, V.Y. Ntsogo Enguene, S.E. Cannella, O. Subrini, A. Hessel, S. Debard, D. Ladant, A. Chenal, Calcium, acylation, and molecular confinement favor folding of Bordetella pertussis adenylate cyclase CyaA toxin into a monomeric and cytotoxic form, J. Biol. Chem. 289 (2014) 30702–30716.
[54] J. Masin, M. Basler, O. Knapp, M. El-Azami-El-Idrissi, E. Maier, I. Konopasek, R. Benz, C. Leclerc, P. Sebo, Acylation of lysine 860 allows tight binding and cytotoxicity of Bordetella adenylate cyclase on CD11b-expressing cells, Biochemistry 44 (2005) 12759–12766.
[55] D.P. O'Brien, S.E. Cannella, A. Voegele, D. Raoux-Barbot, M. Davi, T. Douche, M. Matondo, S. Brier, D. Ladant, A. Chenal, Post-translational acylation controls the folding and functions of the CyaA RTX toxin, FASEB J. 33 (2019) 10065–10076.
[56] V. Havlicek, L. Higgins, W. Chen, P. Halada, P. Sebo, H. Sakamoto, M. Hackett, Mass spectrometric analysis of recombinant adenylate cyclase toxin from Bordetella pertussis strain 18323/pHSP9, J. Mass Spectrom. 36 (2001) 384–391.
[57] S. Bhakdi, N. Mackman, J.M. Nicaud, I.B. Holland, Escherichia coli hemolysin may damage target cell membranes by generating transmembrane pores, Infect. Immun. 52 (1986) 63–69.
[58] A. Ludwig, R. Benz, W. Goebel, Oligomerization of Escherichia coli haemolysin (HlyA) is involved in pore formation, Molecular & general genetics: MGG 241 (1993) 89–96.
[59] G. Menestrina, Escherichia coli hemolysin permeabilizes small unilamellar vesicles loaded with calcein by a single-hit mechanism, FEBS Lett. 232 (1988) 217–220.
[60] J. Vojtova-Vodolanova, M. Basler, R. Osicka, O. Knapp, E. Maier, J. Cerny, O. Benada, R. Benz, P. Sebo, Oligomerization is involved in pore formation by Bordetella adenylate cyclase toxin, FASEB journal: official publication of the Federation of American Societies for Experimental Biology 23 (2009) 2831–2843.
[61] C. Hyland, L. Vuillard, C. Hughes, V. Koronakis, Membrane interaction of Escherichia coli hemolysin: flotation and insertion-dependent labeling by phospholipid vesicles, J. Bacteriol. 183 (2001) 5364–5370.
[62] A. Ludwig, A. Schmid, R. Benz, W. Goebel, Mutations affecting pore formation by haemolysin from Escherichia coli, Molecular & general genetics: MGG 226 (1991) 198–208.
[63] A. Ludwig, M. Vogel, W. Goebel, Mutations affecting activity and transport of haemolysin in Escherichia coli, Mol. Gen. Genet. MGG 206 (1987) 238–245.
[64] C. Schindel, A. Zitzer, B. Schulte, A. Gerhards, P. Stanley, C. Hughes, V. Koronakis, S. Bhakdi, M. Palmer, Interaction of Escherichia coli hemolysin with biological membranes. A study using cysteine scanning mutagenesis, Eur. J. Biochem. 268 (2001) 800–808.
[65] A. Valeva, I. Siegel, M. Wylenzek, T.M. Wassenaar, S. Weis, N. Heinz, R. Schmitt, C. Fischer, R. Reinartz, S. Bhakdi, I. Walev, Putative identification of an amphipathic alpha-helical sequence in hemolysin of Escherichia coli (HlyA) involved in transmembrane pore formation, Biol. Chem. 389 (2008) 1201–1207.
[66] A. Valeva, A. Weisser, B. Walker, M. Kehoe, H. Bayley, S. Bhakdi, M. Palmer, Molecular architecture of a toxin pore: a 15-residue sequence lines the transmembrane channel of staphylococcal alpha-toxin, EMBO J. 15 (1996) 1857–1864.
[67] R. Benz, Channel formation by RTX-toxins of pathogenic bacteria: basis of their biological activity, Biochim. Biophys. Acta 1858 (2016) 526–537.
[68] J. Masin, R. Fiser, I. Linhartova, R. Osicka, L. Bumba, E.L. Hewlett, R. Benz, P. Sebo, Differences in purinergic amplification of osmotic cell lysis by the pore-forming RTX toxins Bordetella pertussis CyaA and Actinobacillus pleuropneumoniae ApxIA: the role of pore size, Infect. Immun. 81 (2013) 4571–4582.
[69] A. Osickova, H. Khaliq, J. Masin, D. Jurnecka, A. Sukova, R. Fiser, J. Holubova, O. Stanek, P. Sebo, R. Osicka, Acyltransferase-mediated selection of the length of the fatty acyl chain and of the acylation site governs activation of bacterial RTX toxins, J. Biol. Chem. 295 (2020) 9268–9280.
[70] R. Osicka, A. Osickova, T. Basar, P. Guermonprez, M. Rojas, C. Leclerc, P. Sebo, Delivery of CD8(+) T-cell epitopes into major histocompatibility complex class I antigen presentation pathway by Bordetella pertussis adenylate cyclase: delineation of cell invasive structures and permissive insertion sites, Infect. Immun. 68 (2000) 247–256.
[71] J. Bellalou, H. Sakamoto, D. Ladant, C. Geoffroy, A. Ullmann, Deletions affecting hemolytic and toxin activities of Bordetella pertussis adenylate cyclase, Infect. Immun. 58 (1990) 3242–3247.
[72] A. Lepesheva, A. Osickova, J. Holubova, D. Jurnecka, S. Knoblochova, C. Espinosa-Vinals, L. Bumba, K. Skopova, R. Fiser, R. Osicka, P. Sebo, J. Masin, Different roles of conserved tyrosine residues of the acylated domains in folding and activity of RTX toxins, Sci. Rep. 11 (2021) 19814.
[73] J. Jumper, R. Evans, A. Pritzel, T. Green, M. Figurnov, O. Ronneberger, K. Tunyasuvunakool, R. Bates, A. Zidek, A. Potapenko, A. Bridgland, C. Meyer, S.A. A. Kohl, A.J. Ballard, A. Cowie, B. Romera-Paredes, S. Nikolov, R. Jain, J. Adler, T. Back, S. Petersen, D. Reiman, E. Clancy, M. Zielinski, M. Steinegger, M. Pacholska, T. Berghammer, S. Bodenstein, D. Silver, O. Vinyals, A.W. Senior, K. Kavukcuoglu, P. Kohli, D. Hassabis, Highly accurate protein structure prediction with AlphaFold, Nature 596 (2021) 583–589.
[74] E.W. Deutsch, N. Bandeira, Y. Perez-Riverol, V. Sharma, J.J. Carver, L. Mendoza, D. J. Kundu, S. Wang, C. Bandla, S. Kamatchinathan, S. Hewapathirana, B.S. Pullman, J. Wertz, Z. Sun, S. Kawano, S. Okuda, Y. Watanabe, B. MacLean, M.J. MacCoss, Y. Zhu, Y. Ishihama, J.A. Vizcaino, The ProteomeXchange consortium at 10 years: 2023 update, Nucleic Acids Res. 51 (2023) D1539–D1548.
[75] Y. Perez-Riverol, A. Csordas, J. Bai, M. Bernal-Llinares, S. Hewapathirana, D. J. Kundu, A. Inuganti, J. Griss, G. Mayer, M. Eisenacher, E. Perez, J. Uszkoreit, J. Pfeuffer, T. Sachsenberg, S. Yilmaz, S. Tiwary, J. Cox, E. Audain, M. Walzer, A. F. Jarnuczak, T. Ternent, A. Brazma, J.A. Vizcaino, The PRIDE database and related tools and resources in 2019: improving support for quantification data, Nucleic Acids Res. 47 (2019) D442–D450.
[76] L. Cane, N.A. Saffioti, S. Genetet, M.A. Daza Millone, M.A. Ostuni, P. J. Schwarzbaum, I. Mouro-Chanteloup, V. Herlax, Alpha hemolysin of E. Coli induces hemolysis of human erythrocytes independently of toxin interaction with membrane proteins, Biochimie. 216 (2023) 3–13.
[77] V.M. Gordon, W.W. Young Jr., S.M. Lechler, M.C. Gray, S.H. Leppla, E.L. Hewlett, Adenylate cyclase toxins from bacillus anthracis and Bordetella pertussis. Different processes for interaction with and entry into target cells, J. Biol. Chem. 264 (1989) 14792–14796.
[78] J. Morova, R. Osicka, J. Masin, P. Sebo, RTX cytotoxins recognize {beta}2 integrin receptors through N-linked oligosaccharides, Proc. Natl. Acad. Sci. U. S. A. 105 (2008) 5355–5360.
[79] W.U. Rahman, A. Osickova, N. Klimova, J. Lora, N. Balashova, R. Osicka, Binding of *Kingella kingae* RtxA Toxin Depends on Cell Surface Oligosaccharides, but Not on beta2 Integrins, Int. J. Mol. Sci. 21 (2020).
[80] C.A. Espinosa-Vinals, J. Masin, J. Holubova, O. Stanek, D. Jurnecka, R. Osicka, P. Sebo, L. Bumba, Almost half of the RTX domain is dispensable for complement receptor 3 binding and cell-invasive activity of the Bordetella adenylate cyclase toxin, J. Biol. Chem. 297 (2021) 100833.
[81] L. Motlova, N. Klimova, R. Fiser, P. Sebo, L. Bumba, Continuous assembly of beta-roll structures is implicated in the type I-dependent secretion of large repeat-in-toxins (RTX) proteins, J. Mol. Biol. 432 (2020) 5696–5710.
[82] G. Chen, H. Wang, L. Bumba, J. Masin, P. Sebo, H. Li, The adenylate cyclase toxin RTX domain follows a series templated folding mechanism with implications for toxin activity, J. Biol. Chem. 299 (2023) 105150.
[83] H. Wang, G. Chen, H. Li, Templated folding of the RTX domain of the bacterial toxin adenylate cyclase revealed by single molecule force spectroscopy, Nat. Commun. 13 (2022) 2784.